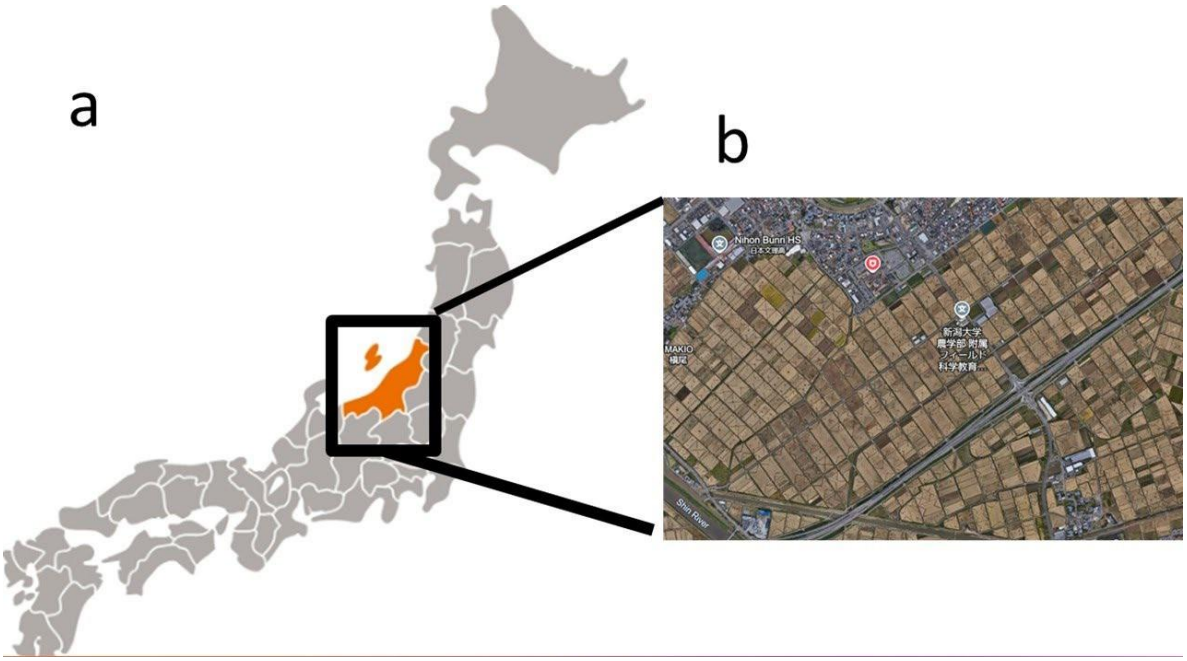


Figure S1*:* Study site location for rice field experiments. (a) Map of Japan highlighting Niigata Prefecture, where the study was conducted. (b) Satellite image of the Shindori paddy fields in Nishi Ward, Niigata, Japan. The field site is part of the Arable Land Production Department, Shindori Station, within the Niigata University Faculty of Agriculture's Field Science Education and Research Centre

Study site location for rice field experiments. (a) Map of Japan highlighting Niigata Prefecture, (a) Map of Japan highlighting Niigata Prefecture, where the study was conducted. (b) Satellite image of the Shindori paddy fields in Nishi Ward, Niigata, Japan (37°51'19"N, 138°57'35"E). The experimental site is part of the Arable Land Production Department at Shindori Station within the Niigata University Faculty of Agriculture's Field Science Education and Research Centre. This region is renowned for its extensive rice production, benefiting from Niigata's favorable climatic conditions, fertile soils, and well-developed agricultural research infrastructure. The site provided a suitable field setting to evaluate the effects of short-term exposure of rice during seedlings to VCs derived from WSFBs on rice growth, yield and grain quality under practical agronomic conditions.

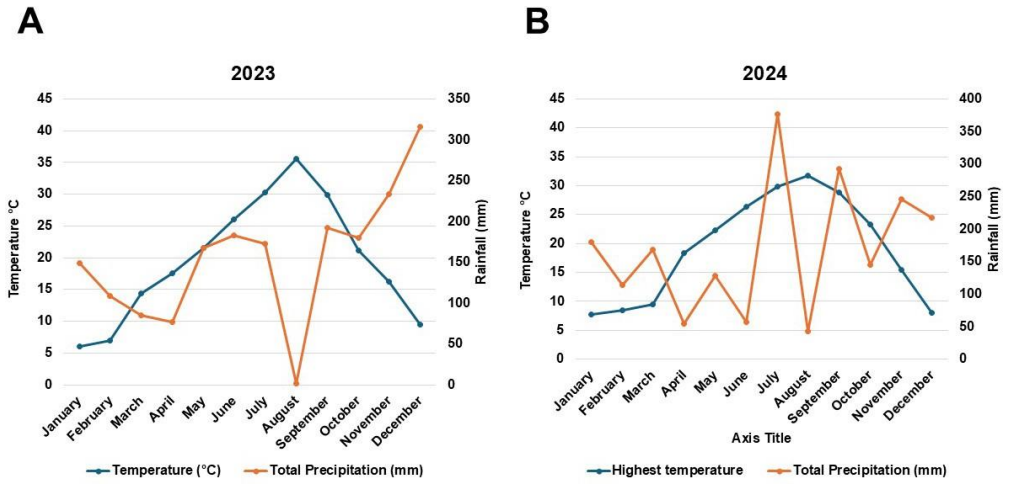


Figure S2: Monthly average daily maximum temperature (°C), **and monthly total of precipitation** (mm) **in Niigata, Japan, during 2023 and 2024**. (A) 2023 and (B) 2024. Both datasets show clear seasonal fluctuations, with temperatures rising from winter to summer and declining toward late autumn, while precipitation varied markedly across months. *Data source: Japan Meteorological Agency (JMA), Niigata WMO Station No. 47604. Accessed from URL:* https://www.data.jma.go.jp/stats/etrn/view/monthly_s3_en.php?block_no=47604&view=13 *(Last accessed on 19th November 2025).*

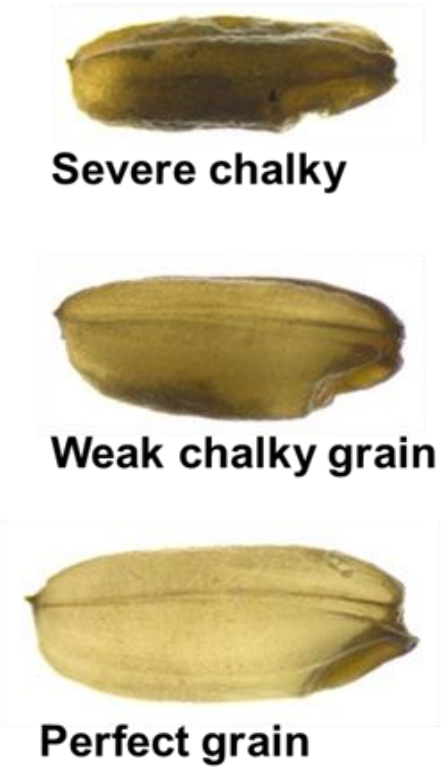


Figure S3: Representative images displaying the chalkiness levels of rice grains. From top to bottom: perfect grains (highly transparent with no cloudy areas), weak chalky grains (cloudy areas like the white back and core, less than 60%), and severely chalky grains (more than 60% cloudy and highly damaged)

Table S1 : Detailed schedule and key activities of rice germination, VCs treatment and paddy field transplantation for rice cultivars 'Koshihikari' and 'Nipponbare' under WSFBs-derived VCs treatment (+VCs) and control (-VCs) conditions

Year	Activity	Period
2023	Seed imbibition, disinfection, and germination	2nd-13th Apr
	WSFBs-VCs treatment and seedling growth	14th Apr - 14th May
	Transplantation to paddy field (Shindori station)	15th May
	Harvest date	30th Sep
2024	Seed imbibition, disinfection and germination	2nd -13th Apr
	WSFBs-VCs treatment and seedling growth	13th Apr - 13th May
	Transplantation to paddy field (Shindori Station)	13th May
	Harvest date	21st Sep

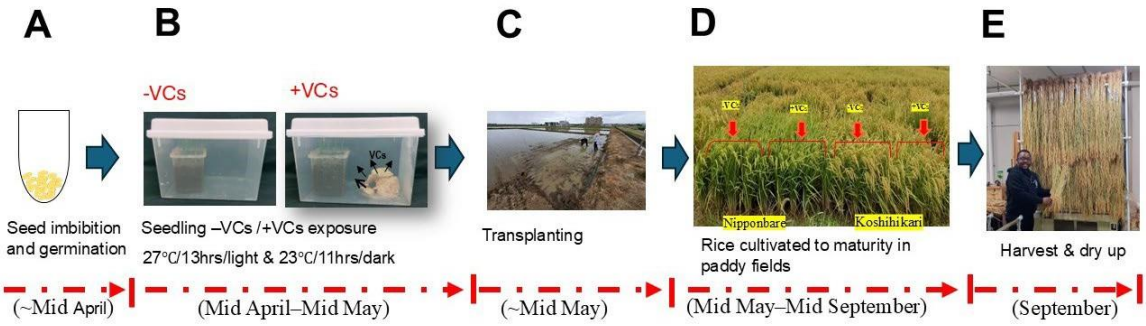


Figure S4. Experimental timeline and workflow of rice seedling stage WSFBs-derived VCs treatment and field level transplantation and evaluation: (A) Seed selection, imbibition, and germination. (B) Seedlings were exposed to WSFBs-derived volatile compounds (+VCs) or left untreated (–VCs) under non-contact conditions. (C) Treated and untreated control seedlings of cultivars 'Nipponbare' and 'Koshihikari' were transplanted into paddy fields. (D) Rice plants were cultivated to full maturity in the fields. (E) After seed maturation, the entire plant was harvested, roots washed and dried at 22-26 °C with humidity below 40% for two months. Yield and grain quality were subsequently evaluated. Blue arrows indicate the experimental progression from seedling treatment through field growth to final harvest.

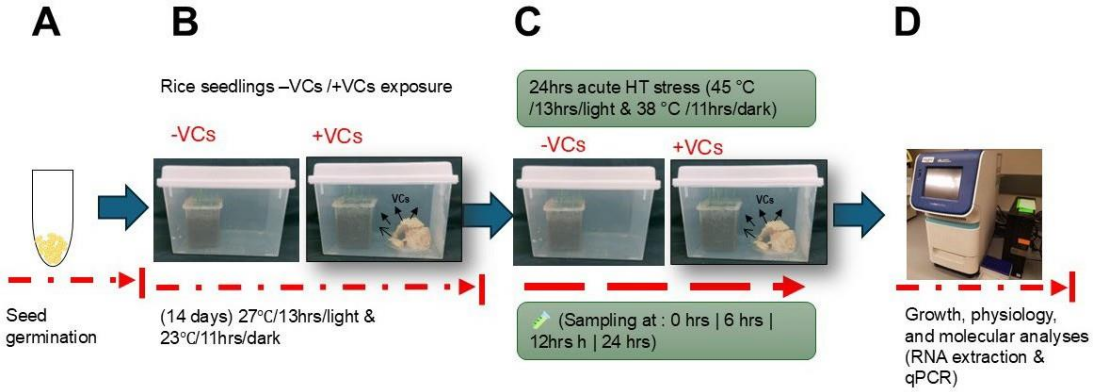


Figure S5. Workflow of the controlled-environment experiment evaluating effects of rice seedlings pre-treatment with WSFBs-derived VCs effects on growth, physiological, and molecular analyses after acute HT stress. The schematic shows (A) seed preparation and germination; (B) seedling exposure to WSFB-derived VCs (+VCs) or untreated control (-VCs) under non-contact conditions; (C) 24-hour acute HT stress treatment (45 °C/13 h light and 38 °C/11 h dark) with sampling for gene expression analysis at 0, 6, 12, and 24 hours post-stress; and (D) quantitative PCR (qPCR) analysis of stress-responsive and hormonal signaling genes. Blue arrows indicate the experimental sequence from seedling treatment through molecular assessment.

Table S2: Growth and physiological parameters of rice seedlings for two weeks treated with WSFBs-VCs (+VCs) and untreated controls (-VCs) then 24 h HT stress treatment. Values represent mean ± SD (n = 5) for cultivar 'Nipponbare" rice seedlings. Significance was determined using Student's t-test ($p < 0.05$ = *, *$p < 0.01$ = **, **$p < 0.001$ = ***, ns = not significant).

Parameter	-VCs	+VCs	Significance
Dry weight (mg)	33.40 ± 5.13	125.20 ± 12.50	***
Shoot height (cm)	35.52 ± 2.15	42.64 ± 1.36	***
Root length (cm)	7.42 ± 1.66	8.50 ± 1.80	ns
SPAD	17.62 ± 5.03	33.36 ± 3.79	**
MDA (nmol g^{-1} FW)	0.02 ± 0.00	0.01 ± 0.00	**
Chlorophyll a (mg g^{-1} FW)	0.58 ± 0.13	1.00 ± 0.14	***
Chlorophyll b (mg g^{-1} FW)	0.42 ± 0.14	0.76 ± 0.17	***
Total chlorophyll (mg g^{-1} FW)	1.00 ± 0.42	1.77 ± 0.15	***

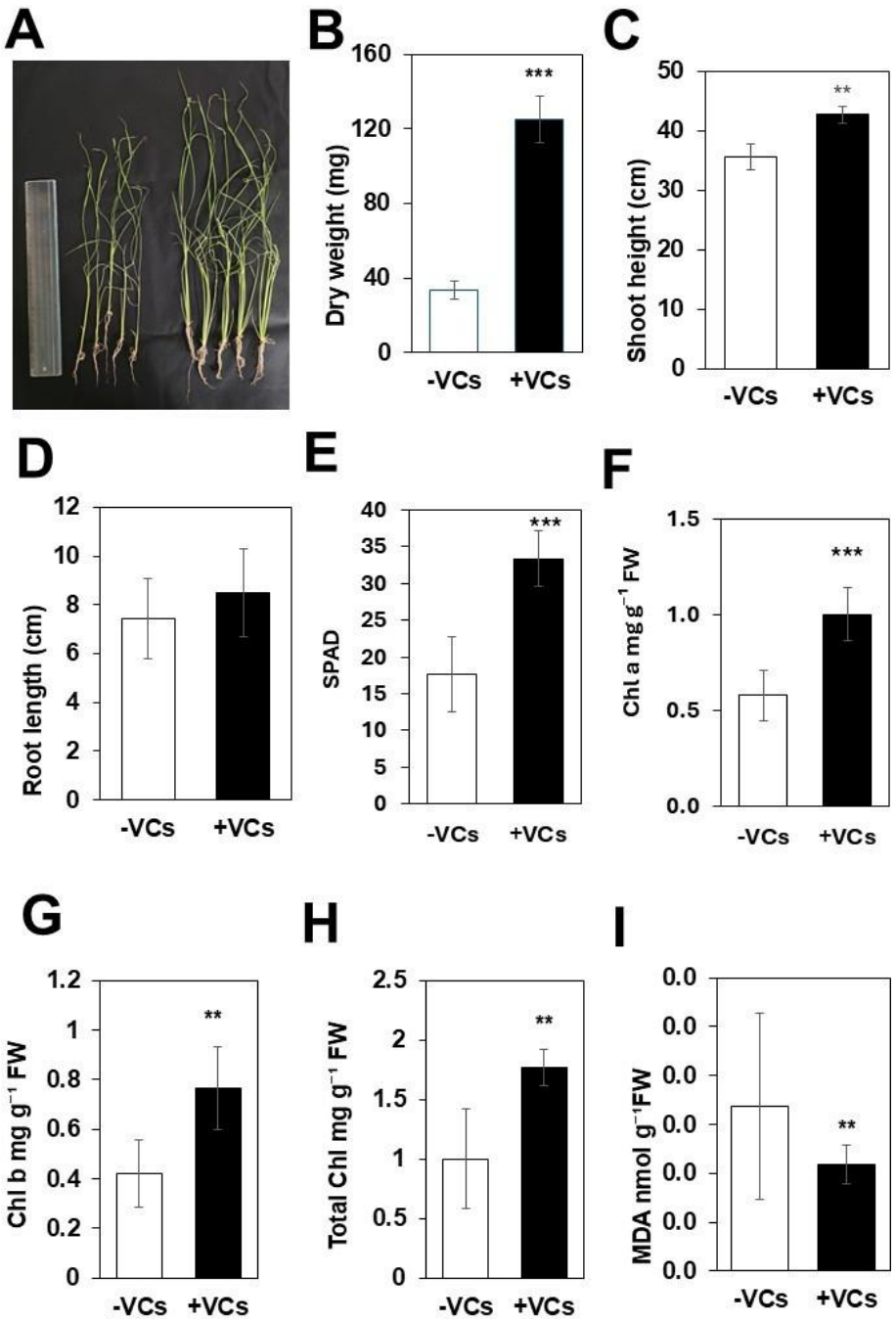


Figure S6. Growth and physiological responses of rice (*Oryza sativa* L. *japonica*, cultivar Nipponbare) seedlings cultivated in a non-contact exposure manner to VCs from WSFBs for 14 days and subsequently exposed to acute HT stress for 24 hrs. (A) Representative phenotype of control (-VCs) and WSFB-derived VCs-treated (+VCs) rice seedlings after HT stress treatment of 45 °C for 13 hrs. in the light followed by 38 °C for 11 hrs. in the dark. Scale bar = 10 cm. (B–I) Quantitative analyses of (B) dry weight, (C) shoot height, (D) root length, (E) SPAD value, (F) chlorophyll a, (G) chlorophyll b, (H) total chlorophyll, and (I) malondialdehyde (MDA) content. Values represent means ± SD (n = 5). Asterisks indicate significant differences according to Student's t-test (*$p < 0.05$; **$p < 0.01$; ***$p < 0.001$).

Table S3. Effects of 31-days exposure to WSFBs-derived volatile compounds (+VCs) on rice seedling growth and biomass accumulation prior to field transplantation. Values are mean ± SD (n = 5). Asterisks indicate significance at $p < 0.05$ and $p < 0.01$ (Student's t-test).

	Nipponbare		Koshihikari	
	-VCs	+VCs	-VCs	+VCs
Dry weight (mg)	157.00±40.87	246.60±73.96*	158.20±24.42	277.60±48.07**
Shoot height (cm)	45.42±2.41	45.12±3.41	47.98±1.85	46.34±4.60
Root length	8.26±1.38	11.20±1.54*	8.74±1.29	8.24±0.73

Exposure of rice seedlings to WSFBs-derived VCs (+VCs) for 31 days promoted improvements in growth and biomass accumulation compared to unexposed controls (-VCs) in both Nipponbare and Koshihikari. The most pronounced responses were observed in dry weight and root length, particularly in Nipponbare, while shoot height remained largely unchanged. These findings indicate that short-term non-contact exposure to WSFBs-derived volatiles enhances early-stage vigor primarily through increased biomass and root system development prior to field transplantation.

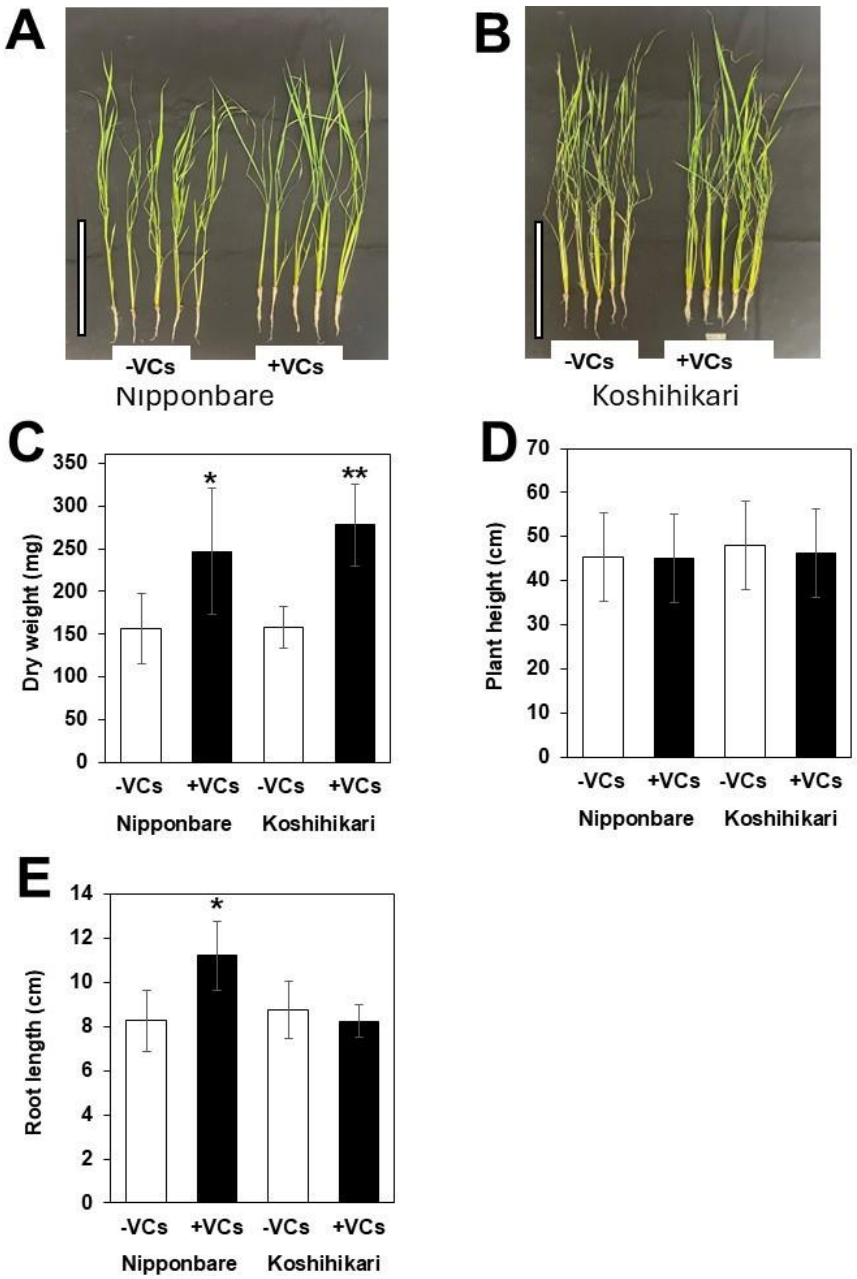


Figure S7: Effects of 31-day exposure to VCs derived from WSFBs on rice seedling growth prior to field transplantation. (A, B) Representative images of *Nipponbare* (A) and *Koshihikari* (B) seedlings exposed to WSFB-derived VCs (+VCs) or unexposed controls (-VCs). Scale bars = 10 cm. (C–E) Quantitative analyses of (C) shoot dry weight, (D) plant height, and (E) root length corresponding to data in Supplementary Table 5. Values represent means ± SD (n = 5). Asterisks indicate significant differences between –VCs and +VCs plants according to Student's t-test (*$p < 0.05$; **$p < 0.01$).

Table S4 : List of primers that were used in this study

Name	Forward primer	Reversed primer
Ubiq5	ACCACTTCGACCGCCACTACT	AGGCCTAAGCCTGCTGGTT
OsRR4	CCGGAGGAGAGAGAGAAAAGAGG	CCAGTTGGTTGGTCCATCAATCTG
OsRR6	GTGTGTTACTCGATCCCCGAGCCT	AAACAGGCTCGGGGATCGAGTAAC
OsRR9	GTGTGGCCGGGGGCCTATTCTTTG	CATGGAACGGAGCCTCTATAGCC
OsRR10	GCTTTCTCCTTGTAGCCTCTTCC	CATGGAACGGAGCCTCTATAGCC
OsGSTU6	CTCCAATCTTCGAGAGACGTG	AGCACACGACAATCTATATGGTT
OsDHAR1	GACGAAGGCAGCTAAGGA	CATGGACCGATCAGATAAAC
OsGRXS17	GAAGCTGAGGAACAACCCG	GCCCAGCTAACTTTGCAACC
OsSLAC1	ATCGCCATCACCAAGGACAG	GCTCTTGGTGATGGACGACAC
OsSNAC1	TGGTGCCCAAGAAAGAATCG	ATGCCCTGGATATCGTCGTAG

WSFBs volatile compounds extraction and chemical analysis

Volatile compounds emitted from waste shiitake fungi beds (WSFBs) were collected using solid-phase microextraction (SPME) fibers (85 μm Carboxen/polydimethylsiloxane, CAR/PDMS and 65 μm polydimethylsiloxane/divinylbenzene, PDMS/DVB; Sigma-Aldrich, St. Louis, MO, USA). Approximately 2.5 g of WSFBs was placed in a 20 mL sealed glass vial, and the SPME fiber was exposed to the headspace for volatile adsorption. The extracted volatiles were subsequently analyzed using a GC-TOF-MS system (JMS-T100GCV, JEOL Ltd., Tokyo, Japan) coupled with an Agilent 7890A gas chromatograph (Agilent Technologies, Tokyo, Japan). The system was equipped with an Agilent G4513A autosampler injector. Mass spectrometric detection was performed under electron ionization (EI) mode.

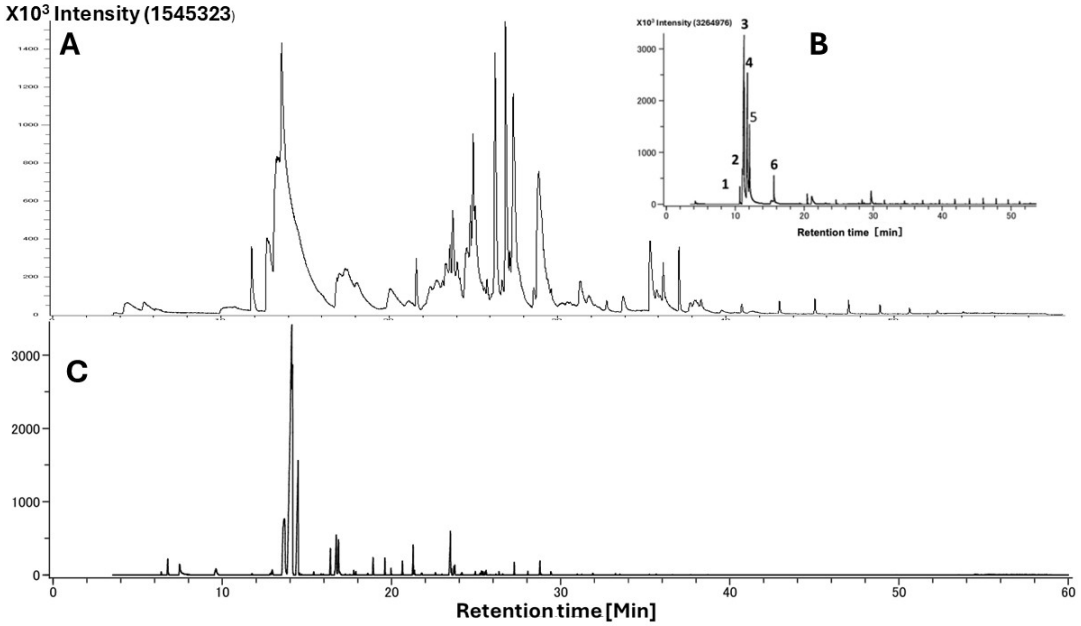


Figure S8: HS-SPME-GC-TOF-MS chromatograms of volatile compounds emifled from waste shiitake fungi beds (WSFBs) at three sampling dates. (A) Sample analyzed on 19 September 2023; (B) sample analyzed on 20 June 2024; and (C) sample analyzed on 25 March 2025. Peak identities for each chromatogram are provided in Table S5. Siloxane peaks were identified as background signals associated with the SPME fiber coating and were excluded from biological interpretation.

Table S5: Comparative profile of major volatile compounds identified in waste shiitake fungi bed (WSFBs) samples across three sampling periods (2023-2025) using HS-SPME-GC-TOF-MS. Compounds were aligned based on retention time and chemical identity, and their occurrence across chromatograms is indicated for Figure S8: (A) 19 September 2023, (B) 20 June 2024, and (C) 25 March 2025. Molecular formulas are included to facilitate comparison of compound classes and chemical features.

Compound name	Approx. RT (min)	A (2023)	B (2024)	C (2025)	Molecular formula	Class
1-Octen-3-one	9.8-10.3	x	✓	✓	$C_8H_{14}O$	Unsaturated ketone
3-Octanone	11.8-12.5	✓	✓	✓	$C_8H_{16}O$	Ketone
1-Octen-3-ol	12.0-12.5	✓	✓	x	$C_8H_{16}O$	Unsaturated alcohol
3-Octanol	12.1-14.0	x	✓	✓	$C_8H_{18}O$	Secondary alcohol
3-Pentanol	~15	✓	x	x	$C_5H_{12}O$	Secondary alcohol
2-Furanmethanol	~18.2	✓	x	x	$C_5H_6O_2$	Heterocyclic alcohol
Oxime-, methoxy-, phenyl-	~21	✓	x	x	$C_8H_9NO_2$	Oxime derivative
1-Hexanol, 2-ethyl-	~25.6	✓	x	x	$C_8H_{18}O$	Alcohol
Oxazin-2-thione derivative	~28.6	✓	x	x	$C_7H_{13}NOS$	Heterocyclic
Dimethyl pentadecanamine	~29.6	✓	x	x	$C_{17}H_{37}N$	Tertiary amine
tau-Cadinol	~36	✓	x	x	$C_{15}H_{26}O$	Terpenoid
2-Octenal	~14.2	x	x	✓	$C_8H_{14}O$	Unsaturated aldehyde
2-Octen-1-ol	~16.2	x	x	✓	$C_8H_{16}O$	Unsaturated alcohol
1-Octanal	~16.4	x	x	✓	$C_8H_{16}O$	Aldehyde
1-Nonanol	~16.5	x	x	✓	$C_9H_{20}O$	Alcohol
2-Undecanone	~22.8	x	x	✓	$C_{11}H_{22}O$	Ketone
3-Methyl-1-heptane	~6.2	x	x	✓	C_8H_{18}	Alkane
Hexanal	~6.4	x	x	✓	$C_6H_{12}O$	Aldehyde
Benzaldehyde	~8.8	x	x	✓	C_7H_6O	Aromatic aldehyde

Key: ✓ present x absent

Note : Siloxane compounds (e.g., Octamethylcyclotetrasiloxane and related cyclic siloxanes) were identified as background peaks originating from the SPME fiber coating material and were excluded from biological interpretation. SPME fiber were fibers 85 μm Carboxen/polydimethylsiloxane, CAR/PDMS (Sigma-Aldrich, St. Louis, MO, USA) for 2023 and 65 μm polydimethylsiloxane/divinylbenzene, PDMS/DVB (Sigma-Aldrich, St. Louis, MO, USA) for 2024 and 2025.